Available online at www.sciencedirect.com

ScienceDirect

Cement and Concrete Research 38 (2008) 667 – 674

Cement and Concrete Research

The mechanism of cesium immobilization in densified silica-fume blended cement pastes

G. Bar-Nes [a,b,*,1], A. Katz [b], Y. Peled [a], Y. Zeiri [a,c]

[a] Department of Physical Chemistry, NRCN, P.O. Box 9001, Beer-Sheva, Israel
[b] Faculty of Civil and Environmental Engineering, Technion, Haifa, Israel
[c] Department of Bio-Medical Engineering, Ben-Gurion University, Beer-Sheva, Israel

Received 18 October 2006; accepted 10 September 2007

Abstract

The role of silica-fume agglomerates, found in densified silica-fume (DSF) pastes, in the immobilization mechanism of Cs ions was studied. Samples of cementitious pastes containing two different forms of silica fume – DSF and raw silica fume (RSF) – were prepared. Leaching experiments showed that both additives reduced the leachability of the metal ion, but the effect of the DSF paste was much stronger. Scanning Electron Microscopy, together with Differential Thermal Analysis, proved that no agglomerated particles were present in the RSF pastes and that the extent of pozzolanic reactivity was higher. We therefore believe that unreacted silica within the DSF agglomerates adsorbs Cs ions and consequently increases their immobilization. Furthermore, this work suggests that during the pozzolanic reaction, a hydrated rim develops around the agglomerate that acts as an additional diffusion barrier for the Cs ions, resulting in an increased efficiency of Cs immobilization.

Keywords: Cement paste; Densified silica fume; Agglomerate; Cesium; Immobilization

1. Introduction

Immobilization of cesium (Cs) ions in cementitious pastes has been studied extensively, mainly with respect to their leaching behaviour [1,2]. In cases in which soluble species such as Cs are incorporated in cementitious pastes, relatively high leaching rates have usually been reported [3,4]. Binding of Cs to the cementitious paste was studied by various researchers [5–7] and was found to have an insignificant effect on the immobilization of the ion. Glasser and Hong [8,9] showed that the binding capacity and bond strength of Cs ions to cementitious pastes are enhanced as the Ca/Si ratio in the paste decreases.

In order to improve the immobilization of this highly soluble ion, pozzolanic additives are commonly used [8,10,11]. During the pozzolanic reaction, amorphous silica originating from the additive, reacts with portlandite, $Ca(OH)_2$, a product of cement hydration, to form additional CSH gel, which has a slightly lower Ca/Si ratio than does the CSH originating from the hydration of cement [12]. The consumption of portlandite does not necessarily result in cessation of reaction. C–S–H is still capable of reacting with silica fume resulting in production of more C–S–H albeit of lower Ca/Si ratio. Excess unreacted silica fume may undergo hydrolysis as well, in which Si–O–Si bond are broken and replaced with Si–OH–Si bonds. This has a potential to generate silica gel, also known to be a strong sorber for Cs.

We have previously shown [13] that the immobilization of Cs ions in cementitious pastes greatly improved due to the addition of densified silica fume (DSF). The combined results from leaching and diffusion tests indicated that the immobilization mechanism is of a chemical nature. Scanning Electron Microscopy (SEM), together with Energy Dispersive Spectroscopy analysis (EDS), revealed the presence of large unreacted

---

* Corresponding author. Tel.: +972 86568717; fax: +972 86568686.
E-mail address: gabi.barnes@gmail.com (G. Bar-Nes).

[1] Present address: Key Center for Polymer Colloids, University of Sydney, NSW 2006, Australia.

0008-8846/$ - see front matter © 2007 Elsevier Ltd. All rights reserved.
doi:10.1016/j.cemconres.2007.09.017

silica-fume agglomerates (typical diameter ~100 μm) in the silica-fume blended cement paste, and EDS analysis showed that the Cs concentration within the agglomerates was significantly higher than in the surrounding paste.

The appearance of such agglomerated particles of silica fume has been already reported in several publications [14,15]. It has been shown that in some cases, the presence of such particles can reduce the positive effect of the silica fume on the microstructure and mechanical properties of the pastes [16]. Furthermore, the presence of silica-fume agglomerates can result in matrix expansion due to the alkali–silica reaction [15,17]. The mechanisms that control the accumulation of Cs ions in the silica-fume agglomerates and their encapsulation are described hereafter.

2. Experimental program

The objective of the present study was to study the role of the agglomerated unreacted silica-fume particles found previously in DSF cementitious pastes [13], in the immobilization mechanism of Cs ions. To achieve this goal, we compared cementitious pastes containing either raw silica fume or densified silica fume. Raw silica fume (RSF) is unprocessed silica-fume particles, roughly 0.1 μm in diameter. To ease handling and avoid health problems, raw silica fume is agglomerated into larger particles, measuring several tenths of a millimeter, designated as densified silica fume (DSF). Batch adsorption tests and leaching tests were performed to compare the binding and immobilization capability of the Cs ions; Single Differential Thermal Analysis (SDTA), Scanning Electron Microscopy (SEM) and Energy Dispersive Spectroscopy analysis (EDS) were used to characterize the composition and microstructure of the pastes.

In order to determine whether the immobilization mechanism is controlled by the adsorption of Cs ions to the silica, i.e. whether it depends on the amount of unreacted silica present in the paste or is controlled by some other mechanism, a paste containing an overdose of raw silica fume was prepared (30% mass replacement of cement). A residual amount of evenly dispersed unreacted silica is expected to remain in this paste upon completion of the pozzolanic reaction with all the portlandite present in the paste. This unreacted silica fume can serve as adsorption sites for the Cs ions and is comparable to the DSF paste in which unreacted silica was found to be present within the agglomerates [13].

2.1. Materials

The cement used was Ordinary Portland cement (OPC) CEM I 52.5N, conforming to EN 197 (Nesher, Israel). The two forms of silica-fume (DSF and RSF) were products of Scancem Chemicals, Norway. Table 1 presents the mineral composition of the different materials used.

Table 1
Mineral composition of the materials — OPC (ordinary Portland cement), DSF (densified silica fume), RSF (raw silica fume) (wt.%)

	OPC	DSF	RSF
CaO	63.23	0.48	0.33
SiO_2	19.15	91.7	92.01
Al_2O_3	5.47	0.75	0.40
Fe_2O_3	2.89	2.33	0.91
MgO	1.32	0.85	1.25
TiO_2	0.40	–	–
K_2O	0.46	1.16	1.40
Na_2O	0.20	0.30	0.39
P_2O_5	0.51	–	–
Mn_2O_3	0.04	–	–
SO_3	2.97	0.25	0.33
Cl	0.01	0.07	0.13
LOI total	3.17	1.78	1.70

2.2. Paste preparation

A series of cementitious pastes blended with either densified or raw silica fume was prepared and compared with unblended Portland cement paste. DSF replacement was 20% by weight, while RSF replacements were 20% and 30%. All pastes were prepared at a constant water to binder (w/b) ratio of 0.45.

The components were mixed in a 5-liter Hobart mixer. Non-radioactive Cs ions (representing the waste ions to be immobilized) were added during paste preparation as a solution of the nitrate salt, $CsNO_3$ (Aldrich chemicals). Pastes of similar composition, excluding the addition of Cs ions, were prepared and used in the batch adsorption experiments.

Specimens prepared for the leaching experiments were cast in plastic molds (diameter 40 mm, height 100 mm), sealed and rotated for the first 24 h to prevent bleeding and segregation. After setting, the samples were removed from the molds, inserted into polypropylene bags, sealed again (to prevent exposure to the atmosphere) and allowed to self-cure at room temperature for 28 days. After curing, the specimens were sliced into 15-mm thick disc shaped samples used for the leaching experiment.

Specimens prepared to study compositional changes during the initial stages of hydration were cast in 25-mm diameter plastic molds. After a desired hydration period, the samples were fractured into small pieces (suitable for the microscopy analysis) and the hydration process was quenched by immersing the samples in isopropanol for an initial 24-hour period, followed by removal of the solvent and a second 5-hour period of immersion in fresh solvent. The samples were then oven-dried at 105 °C for 2 h and the fractured face was gold-coated and prepared for SEM analysis.

2.3. Leaching tests

Leaching tests were performed according to the ANSI/ANS-16.1 (1986) procedure [18], using deionized water as the leachant. The samples contained cesium concentrations of 2.9 mg Cs/g paste. Since the ions were added during the paste preparation stage and the pastes were cured for 28 days prior to the leaching tests, it was assumed that the ions were evenly dispersed and had sufficient time to interact with the paste; i.e. to become chemically bound or incorporated by other effects. The leaching tests were performed using duplicate samples of each of the pastes. Analysis of the leached Cs ions was performed using Inductive Coupled Plasma-Mass Spectroscopy (ICP-MS).

It is assumed that if less than 20% of the leachable species is leached from a uniform, regularly shaped solid, then its leaching

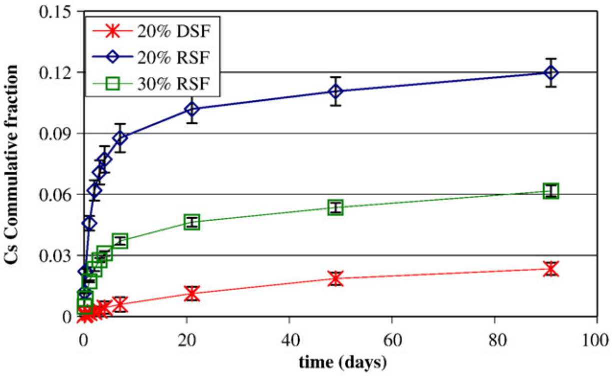

Fig. 1. The cumulative fraction of Cs ions from cementitious pastes blended with DSF and RSF as derived from leaching experiment results.

behavior approximates that of a semi-infinite medium [18]. Under these conditions, the apparent diffusivity of the ion (D_a[Cs]) is calculated using the following equation:

$$D_\mathrm{a} = \pi\left[\frac{(a_n/A_o)}{(\Delta t)_n}\right]^2\left[\frac{V}{S}\right]^2 T, \tag{1}$$

where:

D_a	apparent diffusion coefficient [cm^2/s]
a_n	concentration of the ion released from the specimen during leaching interval n
A_0	total concentration of the ion in the specimen at the beginning of the test
$(\Delta t)_n$	duration of the n^{th} leaching interval [s]
V	volume of the specimen [cm^3]
S	geometric surface area of the specimen [cm^2]
T	cumulative leaching time representing the mean time of the n$^{\mathrm{th}}$ leaching interval [s] calculated from Eq. (2):

$$T = \left[\frac{t_n^{1/2} + t_{n-1}^{1/2}}{2}\right]^2 \tag{2}$$

In cases in which the cumulative fraction exceeds 20%, D_a can be calculated from the shape-specific solution of the mass transport equations using a tabular method given by ANSI/ANS-16.1(1986) [18].

2.4. Batch adsorption experiments

Batch adsorption experiments of Cs ions from a saturated solution of $Ca(OH)_2$ (representing the pore solution) were performed on samples of neat cement paste, blended pastes and neat silica fume (as-received) in its two forms. Cured pastes were grinded and sieved to yield specified particle size (10–20 mesh, i.e. 0.84–2.00 mm).

Samples were allowed to equilibrate for 3 weeks with a saturated solution of $Ca(OH)_2$ containing 1 g/l of Cs ions (as the nitrate salt), at a constant temperature of 30 °C in a closed vessel.

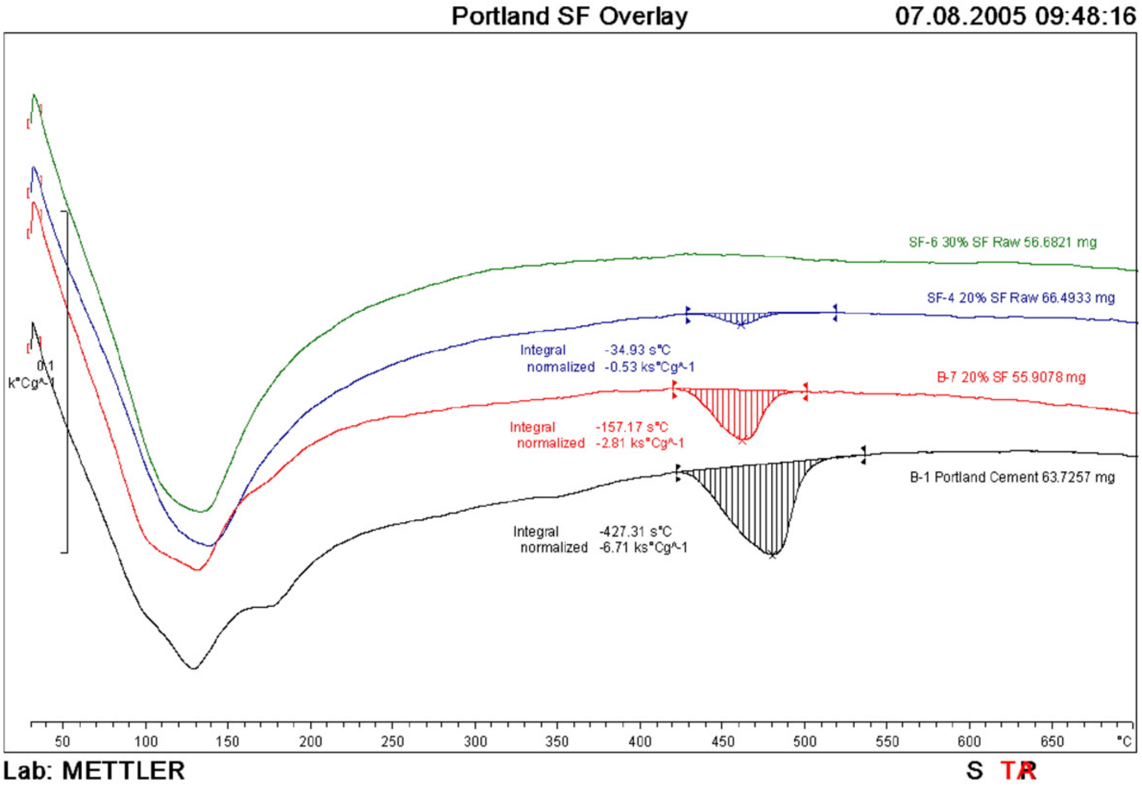

Fig. 2. SDTA results for cementitious pastes blended with silica fume and unblended paste (black —unblended paste, red — 20% DSF, blue — 20% RSF, green — 30%RSF).

Table 2
Calculated areas of the $Ca(OH)_2$ decomposition peak (normalized to cement weight in the sample) and relative pozzolanity of the different pastes

	Integral normalized (ks °C/g cement in sample)	Relative pozzolanity
No additives	9.72	0
DSF 20%	5.11	0.47
RSF 20%	0.96	0.90
RSF 30%	0	1.0

The high concentrations used in the adsorption experiments are mostly due to limitations of the analytical methods used. Even though the difference in the concentrations used in leaching and adsorption experiments is large, we believe that within our experimental concentration ranges the K_d values should not vary significantly with the ion concentration since the concentration of Cs in the pore water of the pastes prepared for the leaching tests increases sharply as water is consumed for the hydration process. Therefore, this difference should not affect our results.

After equilibrium was reached, the liquid phase was separated from the solids by decantation, Cs concentration of the solution was determined and the distribution coefficient (K_d) was calculated.

The distribution coefficient (K_d), describing the ratio between the ion's mass content in the solution and its mass content in the solid phase, was calculated from the following Eq. (3):

$$K_d = \frac{C_0 - C_{sol}}{C_{sol}} \cdot \frac{V}{M} \tag{3}$$

where:

C_0	initial ion concentration
C_{sol}	measured equilibrium concentration of the ion in solution
V	solution volume
M	adsorbent mass

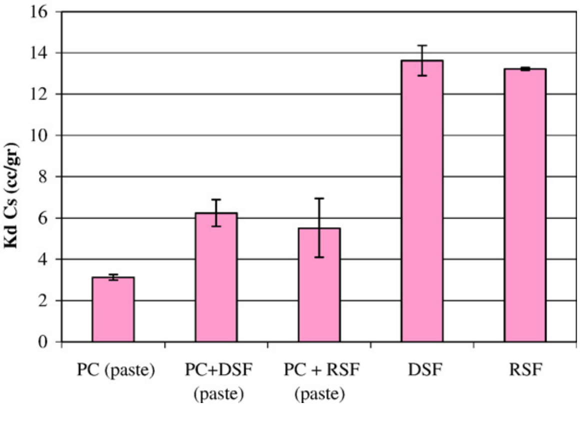

Fig. 3. K_d values for Cs ions in different cementitious pastes and siliceous additives as obtained from batch adsorption experiments.

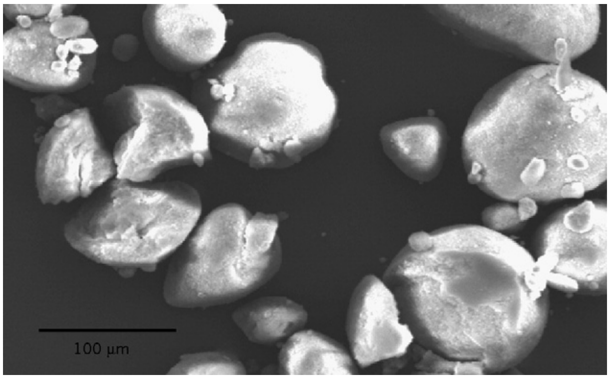

Fig. 4. SEM image of DSF particles.

2.5. Paste characterization

Single Differential Thermal Analysis (SDTA) using Mettler TGA/SDTA851^e was used to determine the calcium hydroxide (CH) content in each of the cured pastes.

In order to quantify the extent of the pozzolanic reaction for each sample as well as the amount of unreacted silica fume remaining in the paste we defined in our work the relative pozzolanicity or the RPR (relative pozzolanic reactivity). The RPR was defined as the relative consumption of CH in the SF blended pastes compared with the unblended paste, as calculated from Eq. (4):

$$RPR = \frac{\left[(CH_{OPC}) - (CH_{SFpaste})\right]}{(CH_{OPC})} \tag{4}$$

where CH_{OPC} represents the integrated area of the $Ca(OH)_2$ peak obtained from the SDTA results for the unblended Portland cement paste and $CH_{SFpaste}$ represents the integrated area of the $Ca(OH)_2$ peak in the SF blended paste.

SEM analysis, together with EDS, was employed to characterize both the local morphology and chemical composition of the different paste samples. This kind of measurement assists in mapping the location of immobilized ions within the paste, provided their local concentration is above the detection limit. In order to study changes in the chemical composition throughout

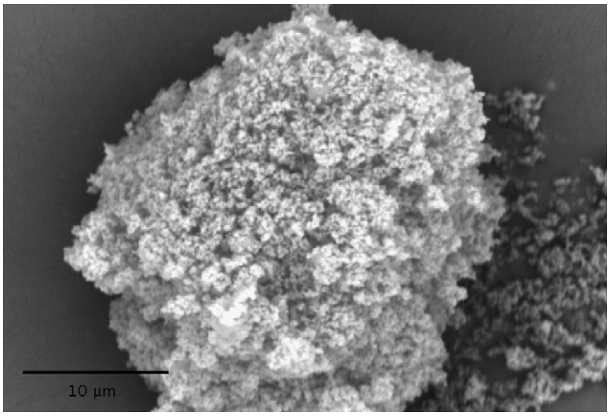

Fig. 5. SEM image of RSF particles.

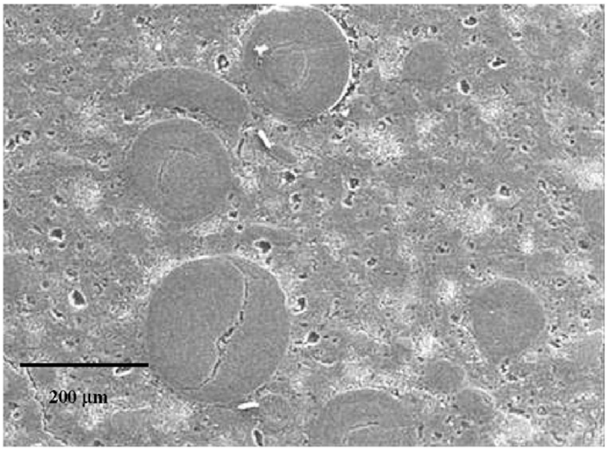

Fig. 6. SEM image of DSF blended paste.

hydration, the hydration of different samples was stopped after 5, 12, and 31 days from the beginning of hydration.

3. Results

3.1. Leaching results

Fig. 1 presents the leaching curves obtained for Cs ions immobilized within the different cementitious pastes blended with SF. A previous study [13] showed that the leachability of Cs ions from unblended cement pastes is quite high, yielding an accumulated released ion fraction of 0.8 at the end of the leaching test (90 days). Fig. 1 shows that in the presence of either forms of SF, leaching of Cs ions is much more restrained. The DSF paste exhibited the highest reduction in Cs leachability, with a released accumulated fraction of less then 0.03 at the end of the experiment. The effect of a 20% addition of RSF was also marked compared with the unblended paste (a released accumulated fraction of 0.12), although less pronounced compared with the DSF blended paste. Leachability values of Cs ions from cementitious samples blended with 30% raw silica fume were in between those of the two other pastes (released fraction of 0.06).

3.2. Thermal analysis results

The different cement pastes were characterized by SDTA to determine the content of CH. Fig. 2 presents SDTA curves for the different pastes (paste composition is indicated on the right hand side of each curve). The wide peak in the temperature range 90–150 °C corresponds to the loss of water from the CSH gel and sulfoaluminates. The peak around 500 °C corresponds to the decomposition of CH [19]. The area under the peak at 500 °C provides a quantitative measure of the extent of the pozzolanic reaction. As can be seen, the 30% RSF paste exhibits no peak in this range, indicating that all of the CH content in this paste has been consumed by the pozzolanic reaction. Table 2 presents the integrated areas under the decomposition peaks, normalized to the cement content in the sample, together with the calculated relative pozzolanity of the pastes.

3.3. Batch adsorption results

Batch adsorption experiments were performed in order to evaluate the K_d values of Cs ions for the cementitious pastes, with and without SF, and for the neat silica-fume additives. Fig. 3 presents the evaluated K_d values. The adsorption of Cs ions by the cementitious paste seems to improve following the addition of both forms of SF. The relatively similar K_d values obtained for the two forms of SF indicate that the SF particles' capability to bind the Cs ion is not affected by their morphology.

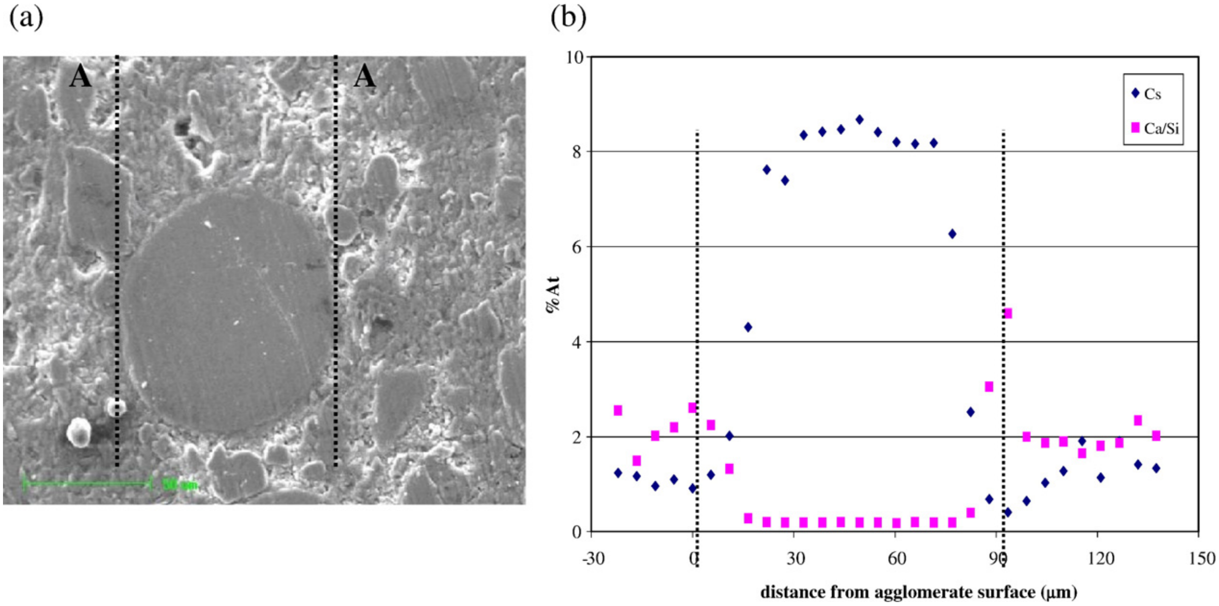

Fig. 7. (a) SEM image of a silica-fume agglomerated cluster. (b) EDS analysis of the Cs ion concentration (at.%) and Ca/Si atomic ratio across the cluster (A–A).

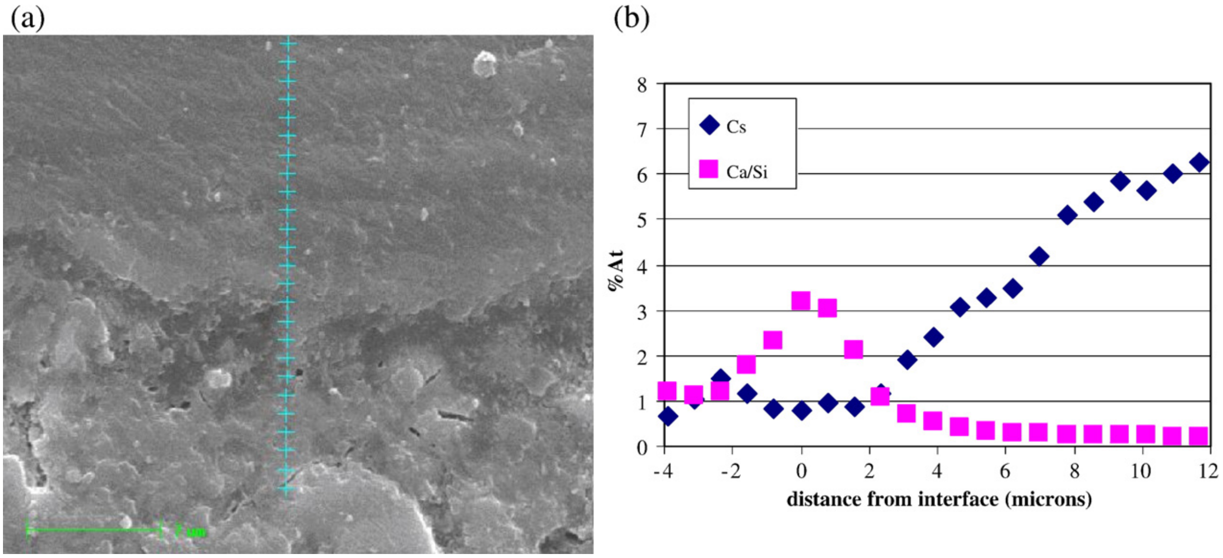

Fig. 8. (a) SEM image of the interface between a silica-fume agglomerated cluster and the paste. (b) EDS analysis of the Cs ion concentration (at.%) and Ca/Si atomic ratio vs. distance from interface.

3.4. Scanning electron microscopy results

Figs. 4 and 5 present SEM images of the two forms of silica fume. The DSF is composed of large agglomerated clusters (with an average diameter of approximately 100 mm) that seem to be tightly packed (Fig. 4). As for the RSF, the individual silica-fume particles are much smaller and even when some agglomeration is observed, the particles still seem to be very loosely bound (Fig. 5).

The SEM image of the DSF blended paste (Fig. 6) shows that the large spherical DSF clusters have not disappeared during paste preparation and are evenly dispersed in the cementitious paste. Such clusters were not detected in the pastes blended with RSF.

Fig. 7a presents the SEM image of a single agglomerated cluster. EDS analysis along line A–A (Fig. 7b) reveals that the particle is composed mainly of silica, with calculated Ca/Si values near 0.2 at the interior of the agglomerated cluster. In comparison, Ca/Si values of 1–2, typical for C–S–H, were measured at different locations of the bulk matrix outside the cluster.

The Cs concentration seems to be inversely proportional to the Ca/Si ratio, with low ion concentrations in the bulk matrix that increase sharply upon entering the agglomerate (Fig. 7b).

Fig. 8a presents an enlargement of the interface between the agglomerated silica-fume cluster and the bulk matrix. A line scan EDS elemental analysis of this interfacial zone (Fig. 8b) shows the presence of a distinct transition zone between the bulk matrix and the silica-fume agglomerate, in which the Ca/Si ratio varies significantly. The Ca/Si ratio increases from ~1.2 in the bulk matrix to ~3 at the interface and then decreases sharply to ~0.2 over a short distance of 5–6 μm upon entering the agglomerate (Fig. 8b.) This relatively high Ca concentration within the transition zone can be related to the accumulation of calcium hydroxide around the SF agglomerate reacting with the silica and leading to the formation of a hydrated rim on the agglomerate surface. The occurrence of hydrated rims with relatively high calcium content surrounding the silica agglomerates has been previously reported by Diamond et al. [17]. This effect could not be checked for systems where the $Ca(OH)_2$ has been totally consumed since for those pastes no agglomerated particles were found and the Ca/Si ratio was found to be constant throughout the paste.

SEM, together with EDS, was used to examine the build-up of this hydrated rim, for 5, 12 and 30-day old partially hydrated pastes. Fig. 9 presents the variation in atomic concentration of Ca as a function of the distance from the agglomerate surface towards its center. Relatively high values of Ca atomic concentration (14–19 at. %) were found near the agglomerate-bulk interface at all ages. This high concentration of Ca at the interface has already been demonstrated for the mature paste in Fig. 8b. In the paste hydrated for 5 days, the Ca concentration decreased sharply to a constant value (4–6 at. %) over a short

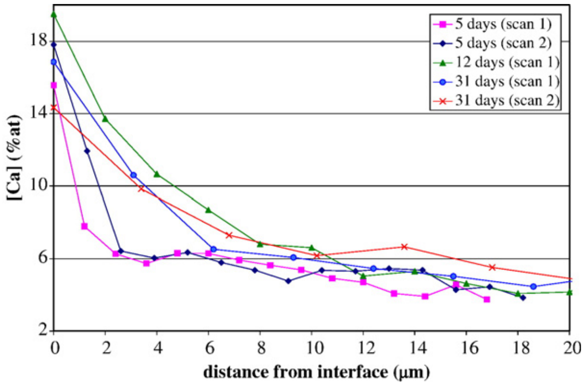

Fig. 9. Ca concentration (at.%) vs. distance from interface towards the center of the DSF agglomerate for different hydration times.

distance of 2–3 μm from the agglomerate surface inward. In pastes hydrated for 12 and 30 days, the Ca concentration gradient was more moderate, reaching a constant Ca concentration at a distance of 6–10 μm inward from the interface.

4. Discussion

The addition of DSF to cementitious pastes was found to be more effective in the immobilization of Cs ions, than the addition of a similar amount of the raw additive (RSF).

SEM observations, together with EDS analysis, revealed the presence of agglomerated silica-fume clusters in the DSF paste, whereas similar clusters were not found in the RSF pastes. The Cs ion concentration was found to increase sharply from low concentrations in the bulk cement to high concentrations in the center of the silica-fume agglomerated clusters. The accumulation of Cs ions within the DSF clusters can be explained in terms of adsorption to the silica, which becomes significant as the Ca/Si ratio decreases, as previously reported by Glasser and Hong [8,9].

A series of experiments was performed in order to determine whether this adsorption is indeed the mechanism that leads to improved immobilization of Cs ions in the DSF blended paste.

Examination of the extent of the pozzolanic reaction in the different pastes (Table 2) shows that an addition of 20% and 30% RSF to the paste results in 0.90 and 1.00 relative pozzolanic reactivity (RPR), respectively. Assuming that the extent of the reaction is linearly dependent on the amount of silica present in the paste and that all of the RSF has reacted, then an addition of 30% RSF leads to a residual amount of ~8% unreacted silica in the paste. The amount of unreacted silica present in the 20% DSF paste was calculated based on the difference between the relative pozzolanity of the 20% RSF and DSF pastes and was found to be ~9.6%, quite similar to that of the 30% RSF paste.

Batch adsorption results show that the distribution coefficients (K_d) of Cs for DSF and RSF (in either neat or blended cementitious pastes) are very similar, indicating that the differences in morphology between the two forms of additive do not seem to have an effect on the binding capability to the ionic species.

Despite the similar contents of unreacted silica, the accumulated leaching fraction of the RSF paste was much larger than that of the DSF paste. This finding suggests that adsorption of Cs ions to the unreacted silica is not the only immobilization mechanism of the ions in the paste, since both the amount of unreacted silica and the binding capabilities of the two pastes are quite similar. Therefore, the large decrease in leachability of the ion from the DSF paste must be the result of a different or an additional mechanism.

EDS results showed the presence of a hydrated rim, formed around the agglomerated clusters of DSF during the hydration of the paste. Based on the measured values of Ca concentration, it seems that the thickness of the hydrated rim increases during the initial days of hydration and then stops growing. Wild et al.[20] showed that at extended curing times, the pozzolanic reaction in DSF pastes seems to be controlled by the build-up of an inhibiting layer of reaction products around the DSF particles, leaving residual unreacted silica in the paste. Even though this end state is probably metastable, we believe that the environmental conditions would not favor the continuation of the pozzolanic reaction. With time the paste is expected to undergo further dehydration which will further slow the diffusion process and inhibit the reaction.

We suggest that Cs ions are adsorbed during the paste preparation (high Cs concentrations were measured within the agglomerates early on in the hydration process), followed by the build-up of a hydration rim surrounding the agglomerated SF particle. This hydration layer, evidenced in this study by EDS analysis, inhibits the completion of the pozzolanic reaction, resulting in a significantly lower relative pozzolanic reactivity for the DSF paste (RPR of 0.47), compared with the 20% RSF paste (RPR of 0.90). We believe that this inhibiting layer can act as an additional diffusion barrier for the chemisorbed Cs ions as well, leading to a significant improvement in the immobilization of Cs ions in the DSF blended cementitious paste compared with the RSF paste.

References

[1] S. Bin-Shafique, J.C. Walton, N. Gutierrez, R.W. Smith, A.J. Tarquin, Influence of carbonation on leaching of cementitious wasteforms, Journal of Environmental Engineering (1998) 463–467 May.

[2] K. Sakr, M.S. Sayed, N. Hafez, Comparison studies between cement and cement–kaolinite properties for incorporation of low-level radioactive wastes, Cement and Concrete Research 27 (1997) 1919–1926.

[3] S. Bagosi, L.J. Csetenyi, Caesium immobilization in hydrated calcium–silicate–aluminate systems, Cement and Concrete Research 28 (12) (1998) 1753–1759.

[4] R.W. Crawford, C. McCulloch, M. Angus, F.P. Glasser, A.A. Rahman, Intrinsic sorption potential of cement components for ^{134}Cs, Cement and Concrete Research 14 (1984) 595–599.

[5] A. Atkinson, A.K. Nickerson, Diffusion and sorption of cesium, strontium, and iodine in water-saturated cement, Nuclear Technology 81 (1988) 100–113.

[6] S. Holgersson, Y. Albinsson, B. Allard, H. Boren, I. Pavasars, I. Engkvist, Effects of gluco-isosaccharinate on Cs, Ni, Pm, and Th sorption onto, and diffusion into cement, Radiochimica Acta 82 (1998) 393–398.

[7] T. Nishi, et al., Effect of porous surface layer on leaching rate of radionuclide from cementitious waste form, Journal of Nuclear Science and Technology 28 (10) (1991) 932–940.

[8] F.P. Glasser, Characterisation of the barrier performance of cements, Materials Research Society Symposium Proceeding 713 (2002) 721–732.

[9] S.-Y. Hong, F.P. Glasser, Alkali binding in cement pastes Part I. The C–S–H phase, Cement and Concrete Research 29 (1999) 1893–1903.

[10] J. Pera, E. Bonnin, Inertization of toxic metals in metakaolin blended cements, environmental issues and waste management technologies in the ceramic and nuclear industries II, Ceramic Transactions 72 (1996) 365–374.

[11] C.E. McCulloch, A.A. Rahman, M.J. Angus, F.P. Glasser, R.W. Crawford, Advances in ceramics: nuclear waste management, American Ceramic Society (1984) 113–128.

[12] V.M. Malhotra, V.S. Ramachandran, R.F. Feldman, P.-C. Aitcin, Condensed silica fume in concrete, CRC Press, Inc., Boca Raton, Florida, 1987.

[13] G. Bar-Nes, "Immobilization of Low Level Waste Containing Strontium and Cesium in Cement Based Systems", PhD Thesis, Submitted to the Technion — Israel Institute of Technology, Haifa, Israel, January 2006.

[14] D. Bonen, S. Diamond, Occurance of large silica fume-derived particles in hydrated cement paste, Cement and Concrete Research 22 (1992) 1059–1066.

[15] S. Diamond, Alkali silica reactions — some paradoxes, Cement and Concrete Composites 19 (1997) 391–401.

[16] J. Yajun, J.H. Cahyadi, Effects of densified silica fume on microstructure and compressive strength of blended cement pastes, Cement and Concrete Research 33 (2003) 1543–1548.

[17] S. Diamond, S. Sahu, N. Thaulow, Reaction products of densified silica fume agglomerates in concrete, Cement and Concrete Research 34 (2004) 1625–1632.

[18] ANSI/ANS-16.1-1986, Measurement of the leachability of solidified low-level radioactive wastes by a short-term test procedure, American Nuclear Society, Illinois, USA, 1986.

[19] W. Sha, E.A. O'Neill, Z. Guo, Differential scanning calorimetry study of ordinary Portland cement, Cement and Concrete Research 29 (1999) 1487–1489.

[20] S. Wild, B.B. Sabir, J.M. Khatib, Factors influencing strength development of concrete containing silica fume, Cement and Concrete Research 25 (7) (1995) 1567–1580.